



Agriculture satellite image segmentation using a modified artificial Hopfield neural network



Rachid Sammouda^{a,*}, Nuru Adgaba^b, Ameer Touir^a, Ahmed Al-Ghamdi^b

^a Department of Computer Science, King Saud University, Riyadh, Saudi Arabia

^b Bee Research Chair, King Saud University, Riyadh, Saudi Arabia

ARTICLE INFO

Article history:

Available online 8 July 2013

Keywords:

Beekeeping
Hopfield neural network
Satellite image segmentation
Pixel clustering

ABSTRACT

Beekeeping plays an important role in increasing and diversifying the incomes of many rural communities in Kingdom of Saudi Arabia. However, despite the region's relatively good rainfall, which results in better forage conditions, bees and beekeepers are greatly affected by seasonal shortages of bee forage. Because of these shortages, beekeepers must continually move their colonies in search of better forage. The aim of this paper is to determine the actual bee forage areas with specific characteristics like population density, ecological distribution, flowering phenology based on color satellite image segmentation. Satellite images are currently used as an efficient tool for agricultural management and monitoring. It is also one of the most difficult image segmentation problems due to factors like environmental conditions, poor resolution and poor illumination. Pixel clustering is a popular way of determining the homogeneous image regions, corresponding to the different land cover types, based on their spectral properties. In this paper Hopfield neural network (HNN) is introduced as Pixel clustering based segmentation method for agriculture satellite images.

© 2013 Elsevier Ltd. All rights reserved.

1. Introduction

Apiculture is one of the most important economic activities for rural communities in Saudi Arabia, while approximately 5000 beekeepers maintain more than million honeybee colonies and produce approximately 900,000 tons of honey annually. In most cases, success in beekeeping depends on the availability of sufficient bee forage in terms of both quality and quantity of nectar and pollen grains. Beekeeping is more dependent on the existing environmental conditions of an area compared with livestock production practices. Unlike other livestock production, it is not possible to keep bees by carrying feeds from other areas, therefore bee forage is considered to be one of the most important elements in the beekeeping industry. In many areas in the Kingdom, bees and beekeepers suffer from seasonal drought, which causes a shortage of bee forage. These conditions drive many beekeepers to move their colonies from one area to another in search of better nectar and pollen sources. Beekeepers concentrate in a few areas in search of a few special species of plants that provide most desired and expensive types of honey. Foraging areas have remained approximately stable in contrast to the constant increase in the number of bee colonies fourfold during the last decade from 270,000 to

more than one million. The result of which is an overpopulation in bee colonies per available foraging areas. However, despite the area's relatively good availability of bee forage, because of seasonal shortages, beekeepers are forced to continually move in search of new bee forage in order to maintain their bee colonies and to obtain a greater honey harvest. The movement of the beekeepers is not systematic or guided with respect to the carrying capacity of the resources and phenology of major bee plants. This leads to serious competition for forage and the subsequent declining of productivity of beekeeping in the region. It is very important to identify and characterize the bee forage of the area in terms of species diversity; population density; ecological distribution; and quality and quantity of nectar and pollen produced by the plants to guide beekeepers.

It is essential to inventory the honeybee populations of the region and determine the optimum bee colony carrying capacity of the different valley areas of Al Baha region as example. Fig. 1 shows a Google map view of the valleys that will be used in our studies. This is used to define a development strategy for beekeeping in the Kingdom of Saudi Arabia using satellite image segmentation.

Segmentation is the process of partitioning an image space into a set of non-overlapping, meaningful, homogeneous regions, where the term "meaningful" is problem-dependent. The success of any subsequent image analysis depends on the quality of the segmentation (Mitra & Kundu, 2011). It refers to the process of assigning a label to every pixel in an image, such that each pixel in the same

* Corresponding author. Tel.: +966 565794451.

E-mail addresses: rsammouda@ksu.edu.sa (R. Sammouda), nurmohammed@ksu.edu.sa (N. Adgaba), touir@ccis.ksu.edu.sa (A. Touir), alkhazim@ksu.edu.sa (A. Al-Ghamdi).

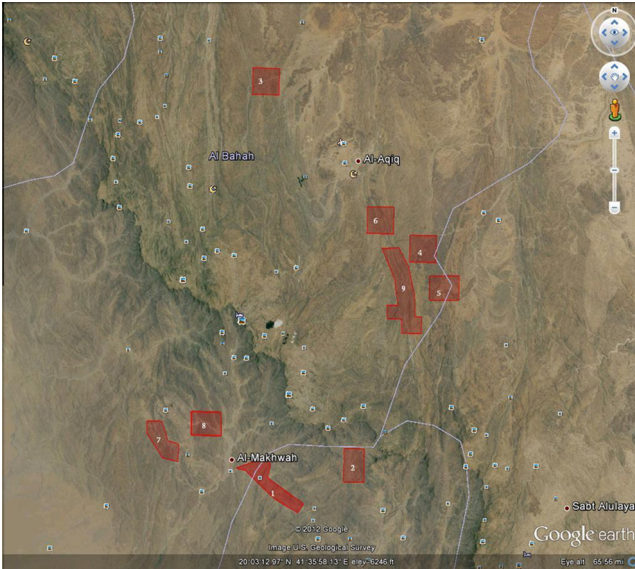


Fig. 1. Google map: localization of the valleys used in this study.

segment (having same label) shares certain visual characteristics – say, color, intensity, and texture. Adjacent regions are ideally expected to be significantly different with respect to these characteristics. Segmentation is an important problem in computer vision and pattern recognition. The goal is to simplify and/or change the representation of an image into something that is more meaningful and easier to analyze (Shapiro & Stockman, 2001). Existing approaches to image segmentation include, among others, methods using thresholds (Mardia & Hainsworth, 1988; Pal, Ghosh, & Uma Shankar, 2000; Harrabi & Braiek, 2012), edges (Perona & Malik, 1990), regions (Banu, 2012; Haris, Efstratiadis, Maglaveras, & Katsaggelos, 1998; Malik, Belongie, Leung, & Shi, 2001), and graphs (Felzenszwalb & Huttenlocher, 2004; Shi & Malik, 2000). One could also formulate segmentation as an optimization problem, with the objective function being something like the inter-cluster variance (Tou & Gonzalez, 1974). Precisely locating the area of interest in an image, in the presence of inherent uncertainty and ambiguity, is a challenging problem in satellite image segmentation. Here one is often faced with a situation that demands proper segmentation.

Clustering can be used to detect, identify and help in the segmentation of an image. Such proper and precise location of an area of interest can significantly aid applications in several domains ranging amongst defence, agriculture, geology, environmental science, etc.

Remotely sensed images are normally poorly illuminated, highly dependent on environmental conditions, and have very low spatial resolution (Mitra & Kundu, 2011). Often a scene contains many ill-defined and ambiguous regions. The grey value assigned to a pixel is also the average reflectance of different types of ground covers present in the corresponding pixel area. Hence assigning unique class labels with certainty is an inherent problem for satellite images. Pixel clustering is one of the fastest and efficient techniques of constituting homogeneous image regions for segmentation. The goal of clustering is to partition N patterns x_k into c desired clusters with high intra-class similarity and low interclass similarity, while optimizing an objective function (Felzenszwalb & Huttenlocher, 2004).

Towards this end, we present in this article the usefulness of the Hopfield neural network (HNN) clustering strategy (Shi & Malik, 2000) for the efficient segmentation of satellite images, based on

their spectral properties. First we present the segmentation technique used in this study, then the analysis process of the segmented images.

2. Proposed method

This section outlines the segmentation technique, which is the first and most important step in any image analysis, and is used in order to prepare an image as an input to an automatic vision system. The purpose of image segmentation is to extract the outlines of different regions in the image, i.e., to divide the image into regions, which are made up of pixels that have some common attributes.

The segmentation problem of an image of N pixels is formulated as a partition of the N pixels among M classes (Sammouda, Sammouda, Niki, & Mukai, 2002) such that the assignment of the pixels minimizes a criterion function. Hopfield neural network has been implemented using C++ programming language and used for the segmentation of cerebral images obtained using magnetic resonance imaging (MRI) (Sammouda et al., 2002). Some limitations have been reported due to the network being stuck in an early local minimum, and this is because the energy landscape in general has more than one local minimum due to the nonconvex nature of the energy surface. In earlier work (Amatur, Piraino, & Takefuji, 1992) the authors have made contributions to the algorithm presented by Sammouda et al. (2002) to alleviate this problem by making HNN converge to a local minimum closer to the global minimum in a pre-specified time. In a comparison of the modified HNN-based segmentation algorithm with those of Boltzmann Machine (BM) and ISODATA, HNN showed a clear advantage in giving crisp segmentation of cerebral MRI images (Amatur et al., 1992). Similar to MRI images, the HNN is used for the segmentation of pathological liver color images (Tou & Gonzalez, 1974).

The HNN structure consists of $N \times M$ neurons with each row representing a pixel and each column representing a cluster. The network is designed to classify the image of N pixels of P features among M classes, such that the assignment of the pixels minimizes the following criterion function:

$$E = \frac{1}{2} \sum_{k=1}^N \sum_{l=1}^M R_{kl}^2 V_{kl}^2 + c(t) \sum_{k=1}^N \sum_{l=1}^M N_{kl} V_{kl} \quad (1)$$

where R_{kl} is considered as the Mahalanobis distance measure between the k th pixel and the centroid of class l , and V_{kl} is the output of the k th neuron. N_{kl} is an $N \times M$ vector of independent high frequency white noise source, used to avoid the network being trapped in early local minimums. The term $c(t)$ is a parameter controlling the magnitude of noise, and is selected in such a way that its value is zero as the network reaches convergence. Minimization is achieved by using HNN and by solving the motion equations satisfying:

$$\frac{\partial U_{kl}}{\partial t} = -\mu(t) \frac{\partial E}{\partial V_{kl}} \quad (2)$$

where U_{kl} is the input of the k th neuron, and $\mu(t)$ is a scalar positive function of time, used to increase the convergence speed of HNN, and is defined by:

$$\mu(t) = t(T_s - t) \quad (3)$$

where t is the iteration step, and T_s is the pre-specified convergence time of the network which has been empirically found to be 120 iterations (Sammouda, Niki, & Nishitani, 1996). The network classifies the feature space, without teacher, based on the compactness of each cluster, calculated using the Mahalanobis distance measure between the k th pixel and the centroid of class l given by:



Fig. 2. Part of a valley in the region of study.



Fig. 3. Segmentation result with two clusters represented with its raw values.

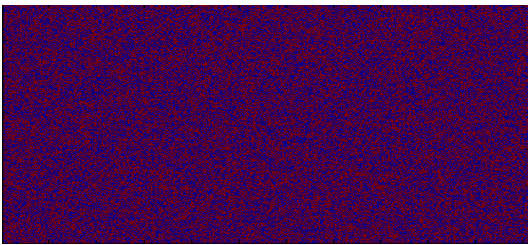


Fig. 4. Segmentation result with two clusters represented in different colors.



Fig. 5. Segmentation result with three clusters represented with its raw values.

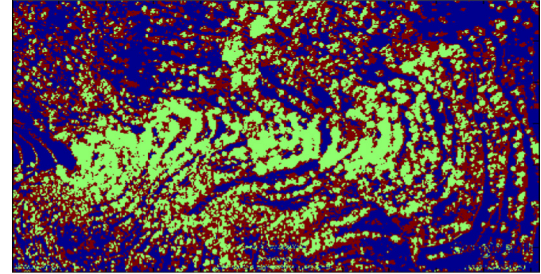


Fig. 6. Segmentation result with three clusters represented in different colors.



Fig. 7. Segmentation result with four clusters represented with its raw values.

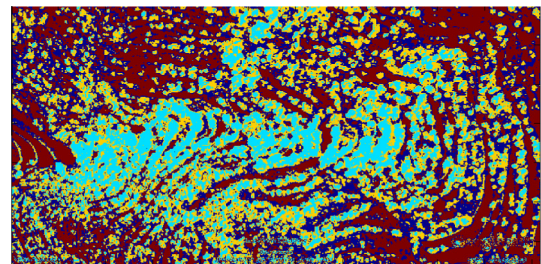


Fig. 8. Segmentation result with four clusters represented in different colors.



Fig. 9. Segmentation result with five clusters represented with its raw values.

$$R_{kl} = \|X_k - \bar{X}_l\| \sum_l^{-1} = (X_k - \bar{X}_l)(X_k - \bar{X}_l)$$

$$1 \leq k \leq N, \quad 1 \leq l \leq M \tag{4}$$

where X_k is the P -dimensional feature vector of the k th pixel (here, $P = 3$ with respect to the RGB, HLS, or HSV color space components), \bar{X}_l is the P -dimensional centroid vector of class l , and \sum_l is the covariance matrix of class l .

2.1. Segmentation algorithm

The segmentation algorithm is as follows:

- Step 1. Initialize the input of the neurons to random values.
- Step 2. Apply the following input–output relation, establishing the assignment of each pixel to only and only one class:

$$V_{km}(t+1) = 1, \quad \text{if } U_{km} = \text{Max}[U_{km}(t), \forall l]$$

$$V_{km}(t+1) = 0, \quad \text{otherwise} \quad 1 \leq k \leq N, \quad 1 \leq l \leq M \tag{5}$$

- Step 3. Compute the centroid \bar{X}_l and the covariance matrix \sum_l of each class l as follows:

$$\bar{X}_l = \frac{\sum_{k=1}^N X_k V_{kl}}{n_l}, \quad 1 \leq l \leq M \tag{6}$$

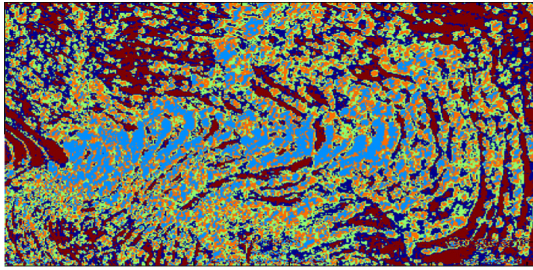


Fig. 10. Segmentation result with five clusters represented in different colors.



Fig. 11. Segmentation result with six clusters represented with its raw values.

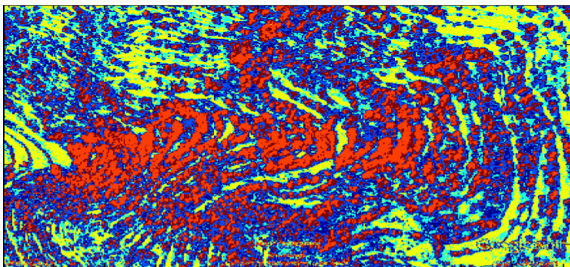


Fig. 12. Segmentation result with six clusters represented in different colors.



Fig. 13. Original satellite image.

$$\sum_l = \frac{[V_{kl}(X_k - \bar{X}_l)(X_k - \bar{X}_l)^T]}{n_l - 1}, \quad 1 \leq l \leq M \quad (7)$$

where n_l is the number of pixels in class l . The covariance matrix is normalized by dividing each of its elements by $\det[\sum_l]_p^{\frac{1}{p}}$

Step 4. Update the inputs of each neuron by solving the set of differential equations in Eq. (2) using Eulers approximation:

$$U_{kl}(t+1) = U_{kl}(t) + \frac{dU_{kl}}{dt}, \quad 1 \leq k \leq N, \quad 1 \leq l \leq M \quad (8)$$

Step 5. If $t < T_s$, go to Step 2, else terminate.



Fig. 14. Segmentation result with two clusters represented with its raw values.

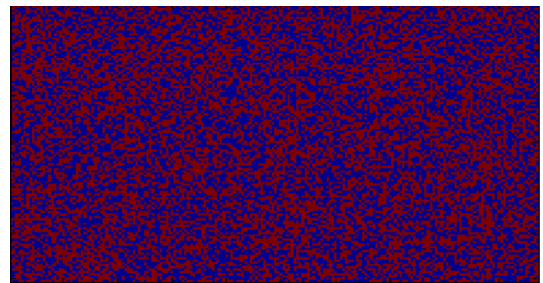


Fig. 15. Segmentation result with two clusters represented in different colors.



Fig. 16. Segmentation result with three represented with its raw values.

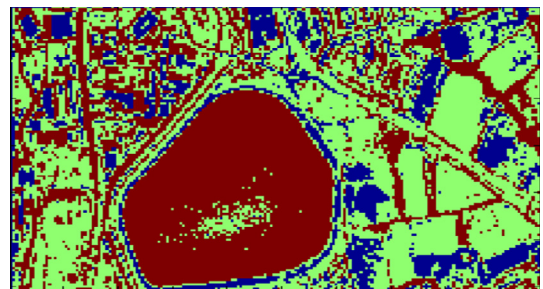


Fig. 17. Segmentation result with three clusters represented in different colors.

3. Result and discussion

We implemented the Hopfield neural network (HNN) clustering algorithm to satellite color images for Al Baha region. The segmentation results as generated on different images. We have used different clusters in order to see the accuracy of the algorithm and the sensitivity of the method. For every pixel in the input image, HNN returns an index corresponding to a cluster. At the last step this method uses the pixel label to separate object in image based on



Fig. 18. Segmentation result with four represented with its raw values.

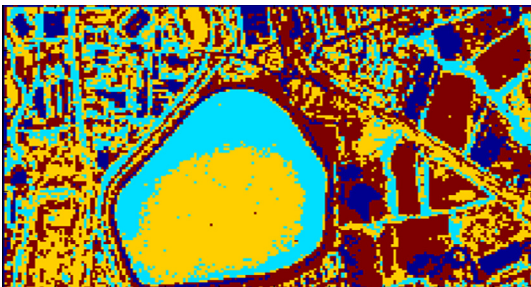


Fig. 19. Segmentation result with four clusters represented in different colors.



Fig. 20. Segmentation result with five represented with its raw values.

the color mean value of the corresponding cluster. Fig. 2 shows the original satellite image. The result when applying two clusters HNN segmentation is represented in Fig. 3 with its raw values and Fig. 4 represented in different color to be distinguishable between different clusters. The result for three clusters segmentation is showed in Figs. 5 and 6. Moreover, the result of four clusters segmentation is represented in Figs. 7 and 8. When applying HNN using five clusters the result in Figs. 9 and 10 are obtained, where Figs. 11 and 12 shows the result when applying HNN with six clusters. We note that using two clusters did not give good results.

The proposed method is also applied on another image which contains different land cover like buildings, water and agriculture area. Fig. 13 shows the original satellite image. The result when applying two clusters HNN segmentation is represented in Fig. 14 with its raw values and Fig. 15 represented in different color to be distinguishable between different clusters. The result for three clusters segmentation is shown in Figs. 16 and 17. Moreover, the result of four clusters segmentation is represented in Figs. 18 and 19. When applying HNN using five clusters the result in Figs. 20 and 21 are obtained, where Figs. 22 and 23 shows the result when applying HNN with six clusters. We note that using two clusters did not give good result, while a good result was obtained when applying four, and five clusters segmentation. More segmentation and analysis results will be presented in future papers with images

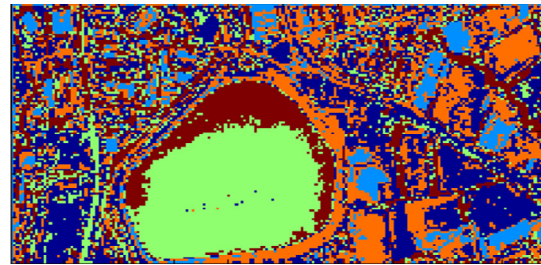


Fig. 21. Segmentation result with five clusters represented in different colors.

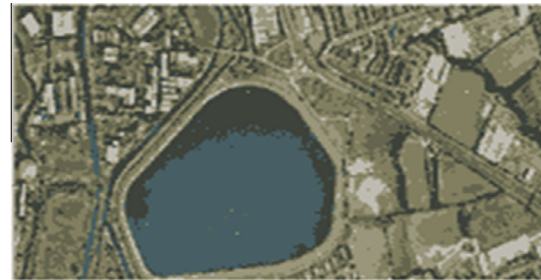


Fig. 22. Segmentation result with six represented with its raw values.

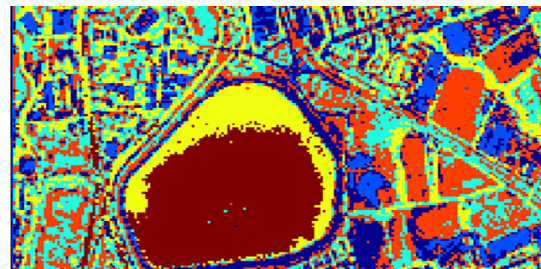


Fig. 23. Segmentation result with six represented with its raw values.

of AlBaha region in Saudi Arabia, collected by GeoEye Satellite with resolution of 0.5 m obtained from the King AbdulAziz City for Science and Technology (KACST).

As can be seen from the presented result, the HNN is giving good result when using three, four, and five clusters. These results will be used to more and fine analysis. In a more extended paper we will apply more analysis of the situation, as we will have the chance to use high resolution multispectral satellite images of Al Baha region.

4. Conclusion

In this paper we presented segmentation result of Al Baha region satellite images obtained using Hopfield neural network clustering algorithm with two, three, four, five and six, clusters and RGB channels data. The result obtained will help beekeepers to be well guided about the actual bee forage areas with specific characteristics like population density, ecological distribution and flowering phenology.

Acknowledgments

This work is supported by the National Plan for Science and Technology, King Saud University, Riyadh, Saudi Arabia under Project Number 11-AGR1750-02.

References

- Amatur, S. C., Piraino, D., & Takefuji, Y. (1992). Optimization neural networks for the segmentation of magnetic resonance images. *IEEE Transactions on Medical Imaging*, 11, 215–220.
- Banu, Sameena (2012). The comparative study on color image segmentation algorithms. *International Journal of Engineering Research an Applications*, 2(4), 1277–1281.
- Felzenszwalb, P. F., & Huttenlocher, D. P. (2004). Efficient graph-based image segmentation. *International Journal of Computer Vision*, 59, 167–181.
- Haris, K., Efstratiadis, S. N., Maglaveras, N., & Katsaggelos, A. K. (1998). Hybrid image segmentation using watersheds and fast region merging. *IEEE Transactions on Image Processing*, 7, 1684–1699.
- Harrabi & Braiek, Ben (2012). Color image segmentation using multi-level thresholding approach and data fusion techniques: Application in the breast cancer cells images. *EURASIP Journal on Image and Video Processing*, 2012, 11.
- Malik, J., Belongie, S., Leung, T., & Shi, J. (2001). Contour and texture analysis for image segmentation. *International Journal of Computer Vision*, 43, 7–27.
- Mardia, K. V., & Hainsworth, T. J. (1988). A spatial thresholding method for image segmentation. *IEEE Transactions on Pattern Analysis and Machine Intelligence*, 10, 919–927.
- Mitra, Sushmita, & Kundu, Partha Pratim (2011). Satellite image segmentation with shadowed C-means. *Information Sciences*, 181, 3601–3613.
- Pal, S. K., Ghosh, A., & Uma Shankar, B. (2000). Segmentation of remotely sensed images with fuzzy thresholding, and quantitative evaluation. *International Journal of Remote Sensing*, 21, 2269–2300.
- Perona, P., & Malik, J. (1990). Scale-space and edge detection using anisotropic diffusion. *IEEE Transactions on Pattern Analysis and Machine Intelligence*, 12, 629–639.
- Sammouda, R., Niki, N., & Nishitani, H. (1996). A comparison of Hopfield neural network and Boltzmann Machine in segmenting MR images of the brain. *IEEE Transactions on Nuclear Science*, 43, 3361–3369.
- Sammouda, M., Sammouda, R., Niki, N., & Mukai, K. (2002). Liver cancer detection system based on the analysis of digitized color images of tissue samples obtained using needle biopsy. *Information Visualization*, 1(2), 130–138.
- Shapiro, L. G., & Stockman, G. C. (2001). *Computer vision*. NJ: Prentice Hall.
- Shi, J., & Malik, J. (2000). Normalized cuts and image segmentation. *IEEE Transactions on Pattern Analysis and Machine Intelligence*, 22, 888–905.
- Tou, J. T., & Gonzalez, R. C. (1974). *Pattern recognition principles*. London: Addison-Wesley.